Experimental Study on the Basic Characteristic of Flux-Path Control Magnetic Suspension

Munehiro Furutachi[*],
07mh219@mail.saitama-u.ac.jp

Shunsuke Inaba[*],

Yuji Ishino[*],
yishino@mech.saitama-u.ac.jp

Masaya Takasaki[*]
masaya@mech.saitama-u.ac.jp

Takeshi Mizuno[*]
mizar@mech.saitama-u.ac.jp

*Department of Mechanical Engineering, Saitama University, 255 Shimo-Okubo, Saitama, 338-8570 Japan

ABSTRACT

In the flux-path control magnetic suspension system, the force acting on the floator is controlled by moving a control plate made of ferromagnetic material, which is located between the permanent magnet and the floator. In this paper, the three-dimensional attractive forces acting on the floator were measured with a manufactured force sensor. The force actuating in the vertical direction is measured with the load cell built in the sensor. The force actuating in the horizontal direction is measured with the plate springs with strain gauges. These measurements clarify the relations between the positions of the control plates and the three-dimensional attractive forces. In addition, stable levitation was achieved by applying PD control. Several dynamic characteristics in the vertical direction were also measured.

INTRODUCTION

The authors have proposed flux-path control magnetic suspension [1]. In the flux-path control magnetic suspension system, the force acting on the floator is controlled by moving a control plate made of ferromagnetic material, which is located between the permanent magnet and the floator. Complete contactless levitation and positioning in the vertical and horizontal directions have been achieved [2], [3]. However, its fundamental properties have not been studied sufficiently. In this paper, a new apparatus with a floator of 1 [kg] is fabricated and the three-dimensional attractive forces acting on the floator are measured. In addition, complete contactless levitation is achieved by applying PD control.

Several dynamic characteristics in the vertical direction are also studied experimentally.

PRINCIPLE OF FLUX-PATH CONTROL MAGNETIC SUSPENSION

Figure 1 shows the principle of flux-path control magnetic suspension. The narrower the distance between the control plates is, the more flux passes through the control plates so that the attractive force acting on the floator is reduced (Fig. 1(a)). In contrast, the wider the distance is, the stronger attractive force acts on the floator (Fig. 1(b)). Stable levitation in vertical direction can be realized by moving the control
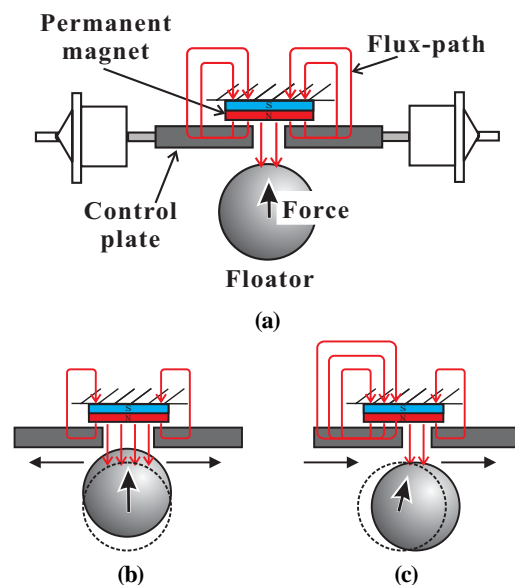

FIGURE 1: Principle of flux-path control magnetic suspension

plates. In addition, control in the horizontal direction also can be realized by moving the control plates in the same direction as shown in Fig. 1(c).

APPARATUS

Figure 2 shows a fabricated experimental apparatus. The size is approximately $300 \times 300 \times 300$ [mm]. It has three flux-path control modules for achieving three-dimensional positions.

In each module, a control plate is attached at the top of the lever. The plate is made of ferromagnetic material and the size is $4 \times 70 \times 25$ [mm]. It controls the flux from the permanent magnet to the floator. The motion of the lever is controlled by a pair of electromagnets located at the bottom of the lever. A gap sensors T_k (k=1, 2, 3) detects the position of the lever.

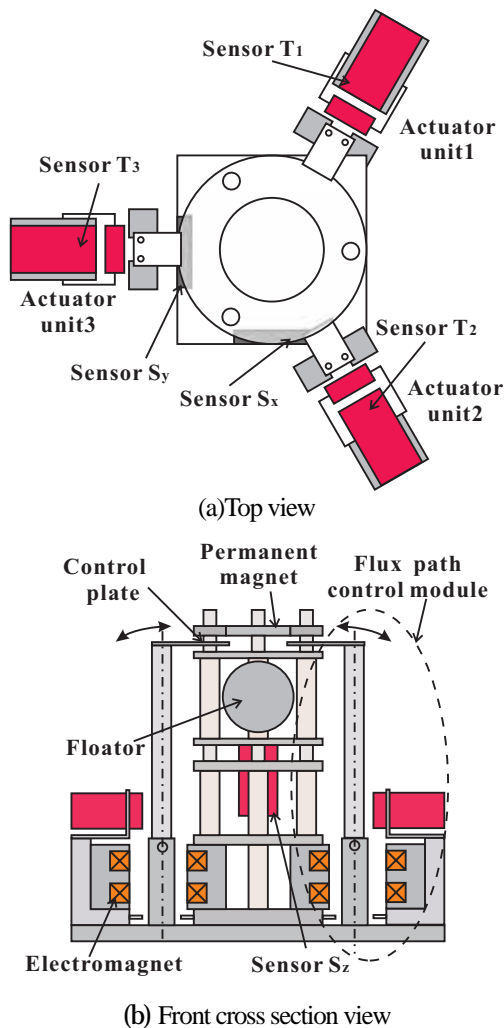The diameter and the mass of the floator are 63 [mm] and 1 [kg] respectively. The three dimensional position of the floator is detected by S_x, S_y and S_z. Figure 3 shows the Photograph of the apparatus.

TWO-AXIS FORCE SENSOR

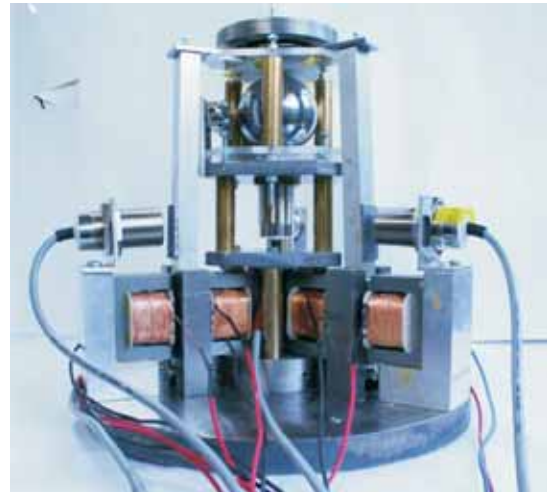Figure 4 shows a manufactured two-axis force sensor for
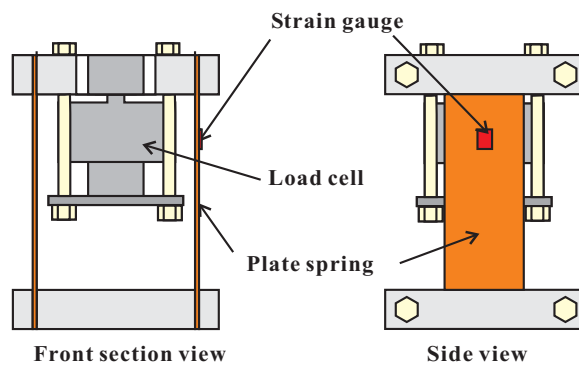

FIGURE 3: Photograph of the apparatus

FIGURE 4: Two-axis force sensor

(a)Top view

(b) Front cross section view

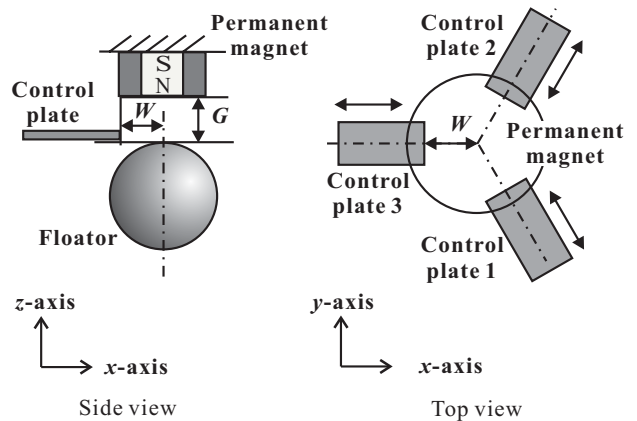**FIGURE 2:** Schematic drawing of the experimental apparatus

FIGURE 5: Definition of coordinate axes and variables

measuring attractive forces acting on the floator. It can measure attractive forces in the vertical and horizontal directions at the same time. The vertical force is measured with the load cell built in the sensor. The horizontal force is measured with the plate springs with strain gauges.

Figure 5 shows the definition of coordinate axes and variables. Three control plates are arranged in a concentric way at every 120 degrees. W is the distance of the control plate from center axis of the floator. G is the gap between the permanent magnet and the floator.

EXPERIMENTAL METHOD

First, the attractive forces F_x and F_z in the x and z-directions are measured with the two-axis force sensor for the following variables:

W: 15 - 22 [mm] and G: 17.4 - 26.4 [mm].

Next, the two-axis force sensor is rotated by 90 degrees and the attractive forces F_y in the y-axis and F_z are measured in the same way. The three components of attractive force are calculated by combining both the measurement results.

EXPERIMENTAL RESULTS

Figures 6 and 7 show the three components of attractive force when one actuator is operated. They show that the smaller G, stronger the attractive force. It also shows that F_x, F_y and F_z is approximately proportional to W. The force can be controlled from 2.1 to 11.3 [N] in the z-direction, and from 0 to 0.35 [N] in the x- and y-directions. Figure 8 shows the three components of attractive force when G is set to be 20.4 [mm] and one actuator is operated. The results are magnified in Fig. 9. The relations expression of F_x, F_y and F_z to W are obtained as

$$F_x = 0.02(W - 15) \qquad [N], \qquad (1)$$
$$F_y = 0.03(W - 15) \qquad [N], \qquad (2)$$
$$F_z = 0.19(W - 15) + 4.4 \qquad [N]. \qquad (3)$$

Figures 10 and 11 show the three components of attractive force when two actuators are operated. The relations of F_x, F_y and F_z to W when $G = 20.4$ [mm] are obtained as

$$F_x = 0.06(W - 15) \qquad [N], \qquad (4)$$
$$F_y = 0.01(W - 15) \qquad [N], \qquad (5)$$
$$F_z = 0.43(W - 15) + 4.4 \qquad [N]. \qquad (6)$$

Comparing Fig. 6 with Fig. 10, we find that the attractive force and its ratio to gap are greater when two actuators are operated. The attractive force constant matrix K_q is defined by

$$F = K_q w, \qquad (7)$$

where

$$F = \begin{bmatrix} F_z \\ F_x \\ F_y \end{bmatrix}, \quad w = \begin{bmatrix} w_1 \\ w_2 \\ w_3 \end{bmatrix}$$
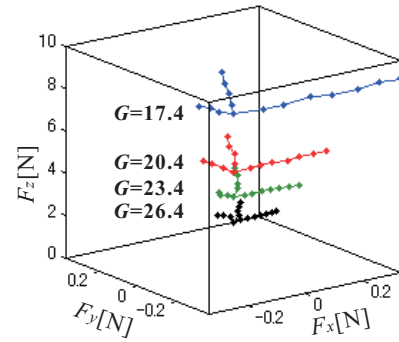
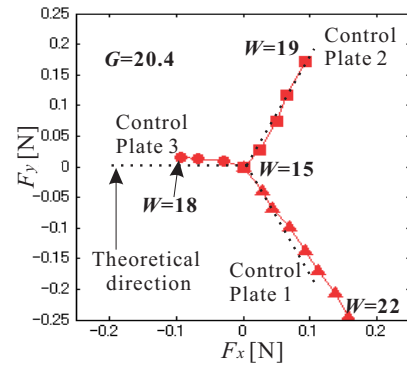**FIGURE 6:** Three components of attractive force acting on the floator when one actuator is operated

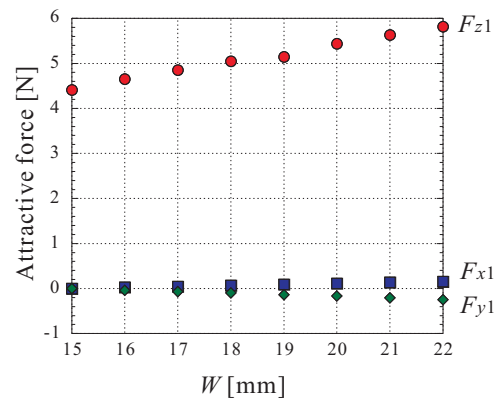**FIGURE 7:** Horizontal components of attractive force when one actuator is operated

FIGURE 8: Three components of attractive force at G=20.4[mm] when one actuator is operated

w_i displacement of control plate i $i=1,2,3$,

$$\boldsymbol{K_q} = \begin{bmatrix} K_{qz1} & K_{qz2} & K_{qz3} \\ K_{qx1} & K_{qx2} & K_{qx3} \\ K_{qy1} & K_{qy2} & K_{qy3} \end{bmatrix}.$$

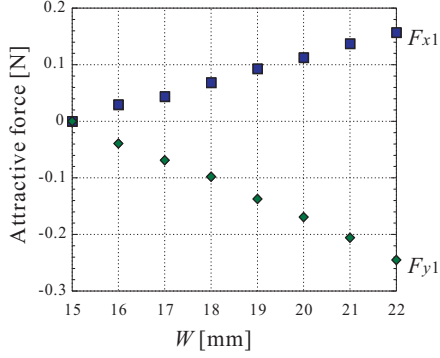From the measurement results, $\boldsymbol{K_q}$ is obtained as given by

FIGURE 9: Horizontal components of attractive force at G=20.4[mm] when one actuator is operated
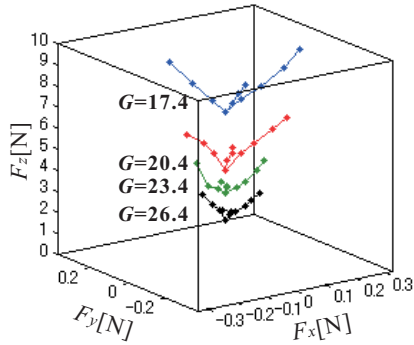

FIGURE 10: Three components of attractive force acting on the floator when two actuators are operated
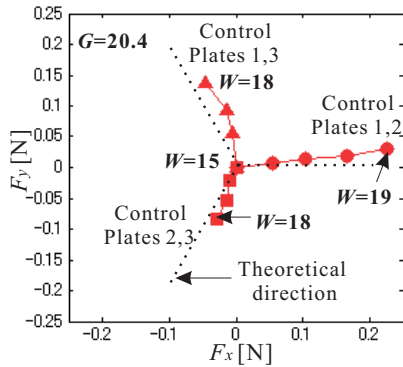

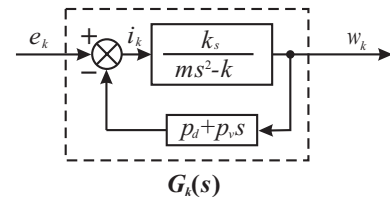**FIGURE 11:**   Horizontal components of attractive force when two actuators are operated

$$\boldsymbol{K_q} = \begin{bmatrix} 0.20 & 0.20 & 0.24 \\ 0.02 & 0.02 & -0.03 \\ -0.03 & 0.04 & 0.01 \end{bmatrix} \quad \text{[N/mm]}. \qquad (8)$$

CONTROL SYSTEM STRUCTURE

In this research, the designed controller has a double-loop structure. In the inner loop, the motion of the flux-path control module is locally fed back. In the outer loop, the displacement of floator in the z-direction is also fed back.

In the inner loop, PD control is applied to provide the flux-path control modules sufficient stiffness and damping property to suspend the floator. In the outer loop, PD control is also applied to stabilize the suspension system.

INNER LOOP

An equation of motion in each flux-path control module is given by

$$m\ddot{w}_k - k_s w_k = k_i i_k \qquad (k=1,2,3) \qquad (9)$$

where m : mass of the control plate with the lever, k_s : force-displacement factor k_i : force-current factor and i_k : control current. When PD control is applied, the control current is given by

$$i_k = -(p_d + p_v \frac{d}{dt})w_k + e_k, \qquad (10)$$

where p_d : proportion gain, p_v : derivative gain and e_k : command signal. The transfer function from e_k to the
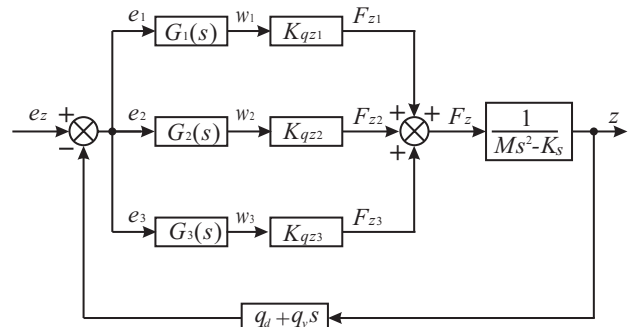

FIGURE 12: Local feedback control

FIGURE 13: Outline of the control system

displacement is obtained as

$$G_k(s) = \frac{b_0}{s^2 + a_1 s + a_0},\qquad(11)$$

where

$$a_1 = \frac{k_i p_v}{m},\qquad(12)$$

$$a_0 = \frac{k_i p_d - k_s}{m},\qquad(13)$$

$$b_0 = \frac{k_i}{m}.\qquad(14)$$

The block diagram of the local feedback is shown by Fig.12.

OUTER LOOP

The motion of the floator in the z-direction is given by

$$M \ddot{z} = F(w_1, w_2, w_3, z) - mg,\qquad(15)$$

where z : displacement of the floator in the z-direction, M : mass of the floator and F : attractive force acting on the floator. Considering the symmetry in structure of the system, we get an equation linearized about the equilibrium state where the gravitation force mg equals the steady magnetic force as

$$M \ddot{z} = K_s z + \mathbf{K_{qz}} \mathbf{w},\qquad(16)$$

where

K_s : force-displacement factor,

$$\mathbf{K_{qz}} = \begin{bmatrix} K_{qz1} & K_{qz2} & K_{qz3} \end{bmatrix}$$
$$= [0.2 \quad 0.2 \quad 0.24] \qquad \text{[N/mm]}.\qquad(17)$$

Control system in the vertical direction of the actual experiment is shown in Fig. 13 where q_d and q_v are proportional and derivative gains in the outer loop.

The displacement signal in the z-direction of the floator is sent to the PD controller. The command signal generated from this controller sent to each module. The attractive forces F_{z1}, F_{z2}, and F_{z3} are changed by moving the control plates.

DIGITAL IMPLEMENTATION

A DSP-based digital controller was used for implementing these controllers. The control period is 100 [μs]. Moreover, an approximation differentiation circuit with the transfer function given by Eq. (18) was built in the digital controller.

$$G_d(s) = \frac{\omega_{n1}\omega_{n2}s}{s^2 + 2\varsigma(\omega_{n1} + \omega_{n2})s + \omega_{n1}\omega_{n2}}.\qquad(18)$$

In the experiment described in the next section, each parameter of the approximation differentiation circuit was set as follows.

$$\omega_{n1} = 200[1/s], \quad \omega_{n2} = 300[1/s], \quad \varsigma = 0.5.$$

POSITIONING IN THE Z-DIRECTION

Figure 14 shows the z-direction displacement of the floator when the command signal e_z is set to be 0.01 to 0.12 [V]. It is found that the position is approximately proportional to the value of command.

STEP RESPONSE IN THE Z-DIRECTION

A rectangular wave with an amplitude e_z =1.4 [V] and a frequency 0.2 [Hz] was inputted as a command signal. Figure 15 shows the displacement when q_d =9.7× 10^2 [A/m] and q_v =29.1 [As/m]. The amplitude of the floator's displacement is about 0.6 [mm].
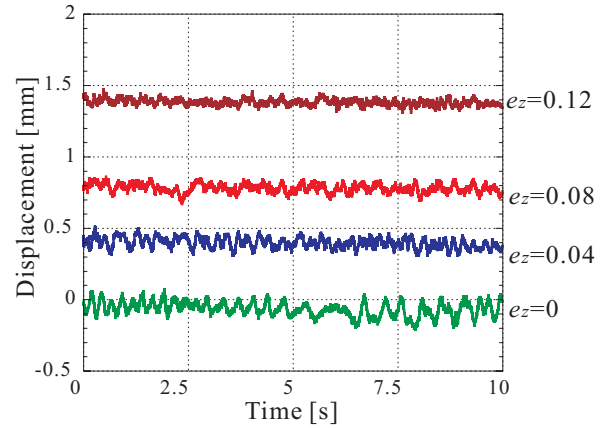

FIGURE 14: Adjustability of the z–direction position by the command signal e_z
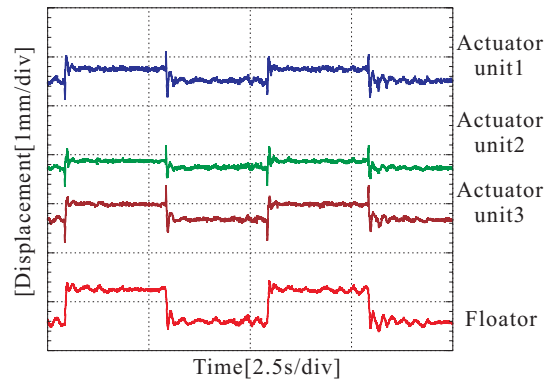

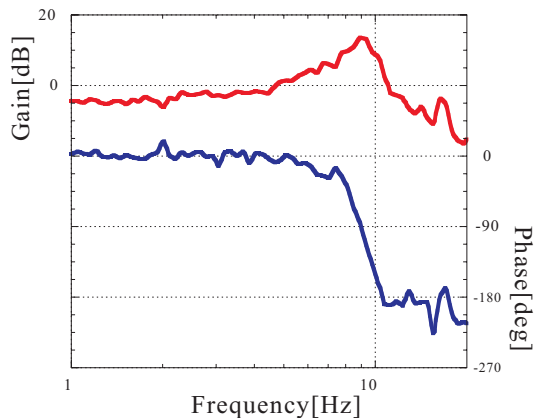**FIGURE 15:** Step response in the z-direction

FIGURE 16: Frequency response of floator in the *z*-direction

FREQUENCY RESPONSE IN THE *Z*-DIRECTION

Figure 16 shows a frequency response in the *z*-direction when $q_d = 9.7 \times 10^2$ [A/m] and $q_v = 29.1$ [As/m]. The input is e_z with an amplitude of 50 [mV] and is the output is displacement *z*. A resonance is observed at a frequency of 8.9 [Hz].

CONCLUSIONS

In flux-path control magnetic suspension system, the three-dimensional attractive forces acting on the floator were measured with two-axis force sensor. The modeling of control system for the vertical motion of the floator was carried out based on these measurement results. In addition, noncontact levitation and positioning in the *z*-direction by the PD control were achieved.

ACKNOWLEDGEMENT

REFERENCES

[1] Jayawant, B.V., Electromagnetic Levitation and Suspension Techniques, Edard Arnold, pp.1-17, 1981.

[2] The Magnetic Levitation Technical Committee of the Institute of Electrical Engineers of Japan (IEE Japan) ed., Magnetic Suspension Technology, (1993), pp.8-13, Corona Publishing Co., LTD.

[3] Higuchi, T. and Oka, K., Reluctance Control Magnetic Suspension System (Suspension System with Permanent Magnet and Linear Actuator), Trans. IEE Japan, Vol. 113-D, No.8, pp.988-994, 1993.

[4] Oka, K., Higuchi, T. and Shiraishi, T., Hanging Type Mag-lev System with Permanent Magnet Motion Control, Trans. IEE Japan, Vol. 119-D, No.3, pp.291-297, 1999.

[5] Ueno, T., Qiu, J. and Tani, J., Magnetic Force Control Based on the Inverse Magnetostrictive Effect, *IEEE Trans. on Magnetics*, Vol.40. No.3, pp.1601-1605, 2004.

[6] Mizuno, T., Hirota, A., Takasaki, M. and Ishino, Y., Flux path Control Magnetic Suspension (1st report : Principle of Suspension), Proceedings of the Kanto Branch Meeting of the Japan Society of Mechanical Engineers (JSME), pp177-178, 2002.

[7] Mizuno, T., Hoshino, H., Ishino, Y. and Takasaki., M., Proposal and Basic Experimental Study of Flux Path Control Magnetic Suspension, Journal of the Japan Society of Applied Electromagnetics and Mechanics, Vol.14, No.3, 2006.

[8] Mizuno, T., Hirai, Y., Ishino, Y. and Takasaki., M., Flux path Control Magnetic Suspension (Development of a System Using Voice Coil Motors), Transactions of the Japan Society of Mechanical Engineers, Series C, Vol.72, No.721, pp.2869-2876, 2006.